4th International Conference on Automation, Control Engineering and Computer Science (ACECS - 2017)
Proceedings of Engineering and Technology – PET
Vol.19, pp.72-77

Nonlinear Control of Voltage Source Inverters in Microgrids

L. Ammeh [1], H. El Fadil [2*], K. Ouhaddach [3]

LGS Laboratory, Ibn Tofail University
BP 242, Av. de L'Université, Kénitra 14 000, MAROC
[1]ammeh.leila@gmail.com
[2]elfadilhassan@yahoo.fr, [3]Ouhaddach.karim.ge2@gmail.com
([*]Corresponding Author)

***Abstract*— Microgrids represent a new and flexible form of electrical networks. This form is based on the use of Distributed Generators which are connected to a microgrid through Voltage Source Inverters (VSI). In this paper, we propose a nonlinear controller that allows the regulation of the output voltage and frequency of a VSI. The system consists of a VSI and an LC filter associated to a coupling inductor. The main objective is to enforce the system output voltage to track a given reference. After the system modeling, the controller is designed using the backstepping technique. Once the control law is elaborated, several simulations are carried out to evaluate the performance of the proposed controller. The simulation results and formal analysis show that the output voltage tracks perfectly the reference voltage with a global asymptotic stability. It is worth mentioning that the designed controller can operate in the both microgrid modes: grid connected mode and islanded mode.**

***Keywords*— Microgrid, distributed Generation, backstepping, VSI, LC filter, coupling inductor, modeling, stability, tracking.**

I. Introduction

In the last decades, the use of Distributed Generation (DG) units has been significantly increased. A DG unit is a generation unit which can produce electricity near customers. Many technologies can be found in DG, for instance, photovoltaic systems, wind turbines, microturbines and fuel cells. Some of these technologies combine the heat and power production (CHP); it is the principal of cogeneration. The increase of the distributed production is owing to the following reasons: the rise of the CO_2 emitted quantity which reached 32381 $MtCO_2$ in 2014 as reported by the International Energy Agency, the global warming, the fossil resource depletion, the considerable increase of the world power consumption and the technological development of DG. The network to which DG units are connected is called a microgrid.

A microgrid can be defined as a cluster of DG units that are generally combined to DC/AC or AC/DC/AC converters [1], storage systems and loads. Compared to a traditional grid, a microgrid has the following advantages: less CO_2 emission, less transmission losses, higher efficiency for energy utilization and flexible installation location [2]. Fig. 1 shows an example of microgrids.

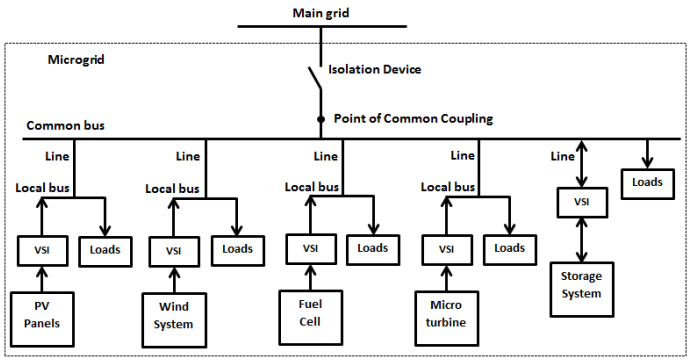

Fig. 1 A microgrid architecture example

A microgrid has two operating modes: grid connected mode where the microgrid is connected to the utility grid and islanded mode where the microgrid operates autonomously disconnected from the main grid. Indeed, if any fault occurs while operating in grid connected mode, microgrid has an ability to disconnect itself, by opening the isolation device in Fig. 1, from the main grid and operate independently supplying its local loads [3].

Controlling voltage and frequency, operating more than one DG unit in islanded mode, power quality issues, implementation and protection represent the most important problems, discussed in [4], that should to be taken in account in a microgrid.

Most of DG units can't be directly connected to the microgrid; they need a DC/AC or AC/DC/AC converter as interface device with the network. The Voltage Source Inverters (VSIs) are the converters widely used in microgrids. Many technologies have been used to control the VSIs as an example: proportional integral (PI), proportional resonant (PR), predictive deadbeat (DB) and hysteresis current controller (HCC). The PI controller has the ability to eliminate the steady state error, however, it has a negative impact on the system overall stability and speed response [5]. The PR controller gives a good tracking to a sinusoidal reference and

This work was supported by the Moroccan Ministry of Higher Education (MESRSFC) and the CNRST under grant number PPR/2015/36.

ISSN 2356-5608

eliminates the steady state error but it resonant frequency requires being identical to the varying grid frequency [6]. The DB controller is widely used for current error compensation, although, it is complicated and sensitive to the system parameters. The HCC controller is simple and gives fast responses, but it leads, in high and variable frequencies, to high current ripples, poor current quality, and difficulties in the output filter design [7].

In this paper, we propose a nonlinear controller using the backstepping technique. The frequency of the output voltage is calculated using the Droop Control Method. We aim to enforce the output voltage to track a given reference.

This paper is structured as follows: section 2 gives the system presentation, section 3 includes the system modeling, section 4 describes the controller design, section 5 presents the simulation results and we end the paper with the conclusion and a reference list.

II. System Presentation

Fig. 2 shows the studied system. It includes the VSI, an LC filter and a coupling inductor.

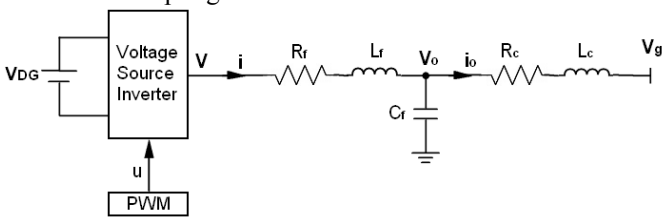

Fig. 2 Single phase diagram of the VSI, the LC filter and the coupling inductor

The LC output filter is used to attenuate the output voltage ripple and to limit the high frequency ripple current of inverter switches [8]. The coupling inductor allows separation of the (sinusoidal) microgrid voltage and the (possibly distorted) grid voltage and also facilitates the control of the real and reactive power exchange between the microgrid and the main grid [9].

R_f , L_f and C_f are, respectively, the resistance, the inductance and the capacitance of the output LC filter. R_c and L_c are, respectively, the resistance and the inductance of the coupling inductor.

III. System Modelling

In Park's d–q frame that rotates synchronously with the inverter output voltage angular speed ω_o , the mathematical model of the system is described by the following equations as in [10]:

$$\frac{di_d}{dt} = -\frac{R_f}{L_f} i_d + \omega_o i_q + \frac{1}{L_f}(v_d - v_{od}) \quad (1)$$

$$\frac{di_q}{dt} = -\omega_o i_d - \frac{R_f}{L_f} i_q + \frac{1}{L_f}(v_q - v_{oq}) \quad (2)$$

$$\frac{dv_{od}}{dt} = \omega_o v_{oq} + \frac{1}{C_f}(i_d - i_{od}) \quad (3)$$

$$\frac{dv_{oq}}{dt} = -\omega_o v_{od} + \frac{1}{C_f}(i_q - i_{oq}) \quad (4)$$

$$\frac{di_{od}}{dt} = -\frac{R_c}{L_c} i_{od} + \omega_o i_{oq} + \frac{1}{L_c}(v_{od} - v_{gd}) \quad (5)$$

$$\frac{di_{oq}}{dt} = -\omega_o i_{od} - \frac{R_c}{L_c} i_{oq} + \frac{1}{L_c}(v_{oq} - v_{gq}) \quad (6)$$

v_d , v_q , i_d and i_q are the d-q axis inverter's voltages and currents, v_{od} , v_{oq} , i_{od} and i_{oq} are the d-q axis output voltages and currents of the studied system, v_{gd} and v_{gq} are the d-q axis grid voltages.

The VSI switching frequency is significantly higher than the power system frequency [11], for this reason, we have used the average version for the above model. The average model is given by the following equations:

$$\dot{x}_1 = -\frac{R_f}{L_f} x_1 + \omega_o x_2 - \frac{1}{L_f} x_3 + \frac{1}{L_f} u_1 \quad (7)$$

$$\dot{x}_2 = -\omega_o x_1 - \frac{R_f}{L_f} x_2 - \frac{1}{L_f} x_4 + \frac{1}{L_f} u_2 \quad (8)$$

$$\dot{x}_3 = \frac{1}{C_f} x_1 + \omega_o x_4 - \frac{1}{C_f} x_5 \quad (9)$$

$$\dot{x}_4 = \frac{1}{C_f} x_2 - \omega_o x_3 - \frac{1}{C_f} x_6 \quad (10)$$

$$\dot{x}_5 = \frac{1}{L_c} x_3 - \frac{R_c}{L_c} x_5 + \omega_o x_6 - \frac{1}{L_c} v_{gd} \quad (11)$$

$$\dot{x}_6 = \frac{1}{L_c} x_4 - \omega_o x_5 - \frac{R_c}{L_c} x_6 - \frac{1}{L_c} v_{gq} \quad (12)$$

Where x_1 , x_2 , x_3 , x_4 , x_5 , x_6 , u_1 and u_2 are, respectively, the average values of i_d , i_q , v_{od} , v_{oq} , i_{od} , i_{oq} , v_d and v_q .

$x = [x_1, x_2, x_3, x_4, x_5, x_6]$ is the state vector.
$u = [u_1, u_2]$ is the input vector.

ω_o is calculated using the droop control method.

Instantaneous active power p is calculated from the measured output voltage and output current as in [12].

$$p = x_3 x_5 + x_4 x_6 \quad (13)$$

The instantaneous active power is passed through a low-pass filter, where ω_c the filter cutoff frequency and s is the Laplace transform operator, to obtain average active power corresponding to the fundamental component; therefore, a high power quality injection is ensured [10].

ISSN 2356-5608

$$P = \frac{s}{s+\omega_c} p \tag{14}$$

The angular frequency of the output voltage is [10]:

$$\omega_o = \omega^* - mP \tag{15}$$

Where ω^* is the nominal frequency set point and m is a static droop gain which can be calculated for a given range of frequency as follows:

$$m = \frac{\omega_{\max} - \omega_{\min}}{P_{\max}} \tag{16}$$

The nonlinearity in (13) makes the studied system a nonlinear system.

IV. Controller Design and Stability Analysis

In this section the backstepping technique, that is described in [13]-[15], is used to enforce the output voltages v_{od} and v_{oq} to track the reference voltages v_{od}^* and v_{oq}^*. The controller is elaborated in two steps for each output voltage.

Let us start by the output voltage v_{od}.

Step 1:

We introduce the first error z_1 defined by

$$z_1 = x_3 - v_{od}^* \tag{17}$$

The aim is to enforce z_1 to vanish.

Differentiating z_1 and substituting from (9), we get

$$\dot{z}_1 = (1/C_f)x_1 + \omega_o x_4 - (1/C_f)x_5 - \dot{v}_{od}^* \tag{18}$$

In (18), $(1/C_f)x_1$ stands as a virtual control input, to which a stabilizing function α_1 is associated.

Furthermore, z_1 vanishes if

$$(1/C_f)x_1 = \alpha_1 \tag{19}$$

To enforce z_1 to vanish, we can choose

$$\dot{z}_1 = -c_1 z_1 \quad , \quad c_1 > 0 \tag{20}$$

c_1 is a design parameter.

From (18), (19) and (20), we get

$$\alpha_1 = -\omega_o x_4 + (1/C_f)x_5 + \dot{v}_{od}^* - c_1 z_1 \tag{21}$$

A second tracking error z_2 is introduced and defined as

$$z_2 = (1/C_f)x_1 - \alpha_1 \tag{22}$$

If z_2 vanishes, then z_1 vanishes.

Substituting $(1/C_f)x_1$ in (18) and using (21) and (22), we get

$$\dot{z}_1 = z_2 - c_1 z_1 \tag{23}$$

Step 2:

Let us differentiate z_2

$$\dot{z}_2 = (1/C_f)\dot{x}_1 - \dot{\alpha}_1 \tag{24}$$

Substitute in (24) and using (7), (10), (11), (21) and (23)

$$\dot{z}_2 = \frac{1}{C_f L_f} u_1 + \beta_1(x) + \frac{1}{C_f L_c} v_{gd} - \ddot{v}_{od}^* + c_1 z_2 - c_1^2 z_1 \tag{25}$$

Where

$$\beta_1(x) = \beta_{11} x_1 + \beta_{12} x_2 + \beta_{13} x_3 + \dot{\omega}_o x_4 + \beta_{14} x_5 - \beta_{12} x_6 \tag{26}$$

With

$$\beta_{11} = -R_f/(C_f L_f) \tag{27}$$

$$\beta_{12} = 2\omega_o / C_f \tag{28}$$

$$\beta_{13} = -(\omega_o^2 + 1/(C_f L_c) + 1/(C_f L_f)) \tag{29}$$

$$\beta_{14} = R_c/(C_f L_c) \tag{30}$$

In the new coordinates (z_1, z_2), the controlled system is represented by (23) and (25).

Let us define the Lyapunov function as

$$V_1 = 0.5(z_1^2 + z_2^2) \tag{31}$$

The time derivative of V_1 along the (z_1, z_2) trajectory using (23) is:

$$\dot{V}_1 = -c_1 z_1^2 + z_2(\dot{z}_2 + z_1) \tag{32}$$

To have $\dot{V} \le 0$, we choose

$$\dot{z}_2 + z_1 = -c_2 z_2, \quad c_2 > 0 \tag{33}$$

c_2 is a design parameter.

$$\dot{V}_1 = -c_1 z_1^2 - c_2 z_2^2 \tag{34}$$

From (25) and (33), we get the first control law u_1:

$$u_1 = C_f L_f \left[z_1(c_1^2 - 1) - z_2(c_1 + c_2) - \beta_1(x) - (1/(C_f L_c))v_{gd} + \ddot{v}_{od}^* \right] \tag{35}$$

We follow the same steps to enforce x_4 to track v_{oq}^*, with the tracking errors:

$$z_3 = x_4 - v_{oq}^* \tag{36}$$

$$z_4 = (1/C_f)x_2 - \alpha_2 \tag{37}$$

The stabilizing function is:

$$\alpha_2 = \omega_o x_3 + (1/C_f)x_6 + \dot{v}_{oq}^* - c_3 z_3 \tag{38}$$

The Lyapunov function is:

$$V_2 = 0.5(z_3^2 + z_4^2) \tag{39}$$

$$\dot{V}_2 = -c_3 z_3^2 - c_4 z_4^2 \tag{40}$$

c_3 and c_4 are design parameters.

The second control law u_2 is:

$$u_2 = C_f L_f \left[z_3(c_3^2 - 1) - z_4(c_3 + c_4) - \beta(x) - (1/(C_f L_c))v_{gq} + \ddot{v}_{oq}^* \right] \tag{41}$$

Where

ISSN 2356-5608

$$\beta_2(x) = -\beta_{12}x_1 + \beta_{11}x_2 - \dot{\omega}_o x_3 + \beta_{13}x_4 + \beta_{12}x_5 + \beta_{14}x_6 \quad (42)$$

$\beta_{11}, \beta_{12}, \beta_{13}$ and β_{14} are defined by (27)-(30).

Proposition

Consider the closed loop system consisting of the system (7)-(12) and the control laws (35) and (41). In the coordinates (z_1, z_2, z_3, z_4), the closed loop undergoes the following equation:

$$\begin{bmatrix} \dot{z}_1 \\ \dot{z}_2 \\ \dot{z}_3 \\ \dot{z}_4 \end{bmatrix} = \begin{bmatrix} -c_1 & 1 & 0 & 0 \\ -1 & -c_2 & 0 & 0 \\ 0 & 0 & -c_3 & 1 \\ 0 & 0 & -1 & -c_4 \end{bmatrix} \begin{bmatrix} z_1 \\ z_2 \\ z_3 \\ z_4 \end{bmatrix} \quad (43)$$

Where the design parameters (c_1, c_2, c_3, c_4) are positive and freely chosen. Hence, the error system (43) is globally asymptotically stable. It follows that:

i) All signals in closed loop are bounded,

ii) The tracking errors $z_1 = x_3 - v_{od}^*$ and $z_3 = x_4 - v_{oq}^*$ vanish.

Proof

Let us consider the following Lyapunov function candidate:

$$V = V_1 + V_2 = 0.5(z_1^2 + z_2^2 + z_3^2 + z_4^2) \quad (44)$$

Its time derivative, using (34) and (40), is

$$\dot{V} = -c_1 z_1^2 - c_2 z_2^2 - c_3 z_3^2 - c_4 z_4^2 \quad (45)$$

Since $V > 0$ and $\dot{V} \le 0$, the (z_1, z_2, z_3, z_4) system is globally asymptotically stable.

V. Simulation Results

The designed controller performance is evaluated using Matlab/Simulink. The system and the controller are modelled based on the scheme of Fig. 3.

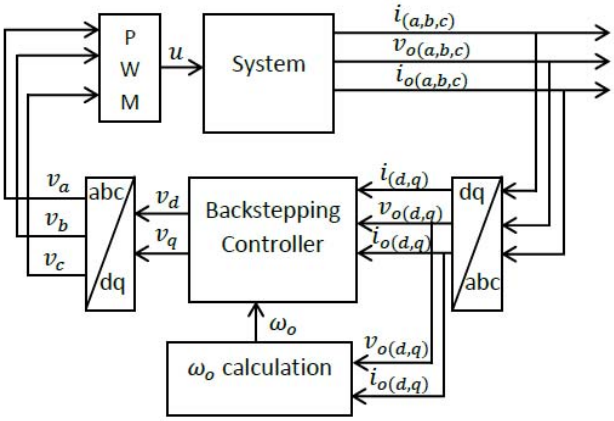

Fig. 3 The simulation model for the studied system

The system and the controller parameters are given in Table 1.

TABLE I
SYSTEM AND CONTROLLER PARAMETERS

$L_f = 1.5mH$	$R_c = 0.05\Omega$	$c_1 = 1000$
$R_f = 0.15\Omega$	$m = 1.33e^{-4} rad/s/W$	$c_2 = 1000$
$C_f = 45\mu F$	$f = 50Hz$	$c_3 = 1000$
$L_c = 0.53mH$	$\omega_c = 30rad/s$	$c_4 = 1000$

The simulation parameters are considered as in [9] and [10].
In this section many simulations have been carried out to ensure that the proposed controller enforce the output voltage to track the reference; the reference voltage is set to $325\sin(\omega t)$.

Fig. 4 shows the system behaviour in grid connected mode with an undistorted grid voltage. The grid voltage is set to $325\sin(\omega t)$.

Fig. 5 gives the system response in grid connected mode with a distorted grid voltage which is set to $325\sin(\omega t) - 32.5\sin(3\omega t) - 32.5\sin(5\omega t)$. The distorted grid voltage can be seen in Fig. 6.
Fig. 7 illustrates the system behaviour in islanded mode.

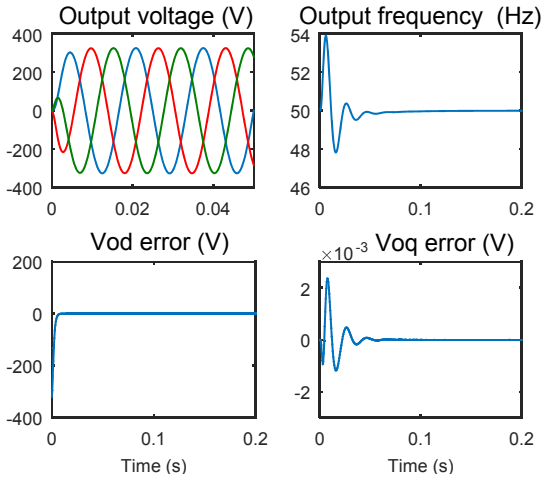

Fig. 4 The system behaviour in grid connected mode with an undistorted grid voltage

ISSN 2356-5608

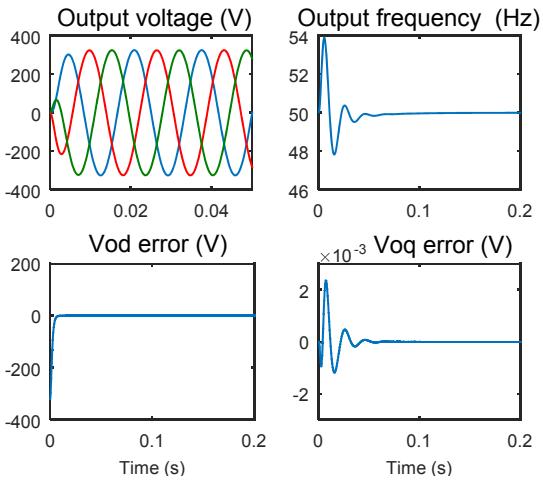

Fig. 5 The system behaviour in grid connected mode with a distorted grid voltage

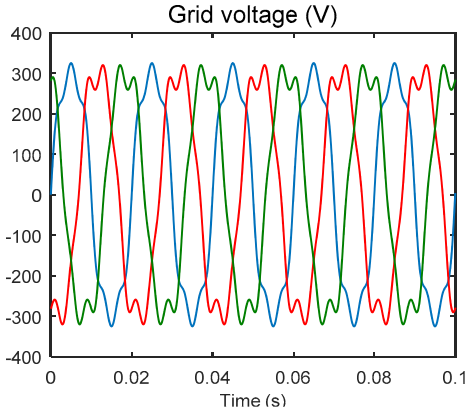

Fig. 6 The distorted grid voltage

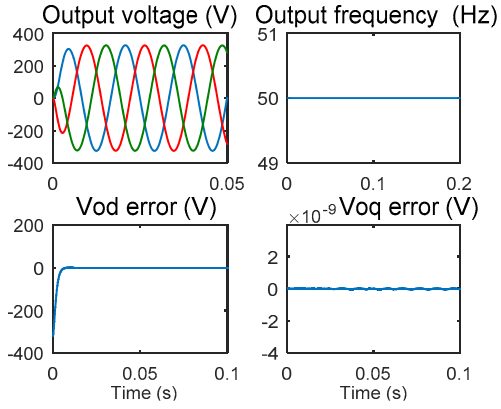

Fig. 7 The system behaviour in islanded mode

In all previous simulations, that have been carried out in grid connected mode and islanded mode, the output voltage of the system tracks perfectly the reference voltage and the steady state is achieved after a very short time which is about 15.22ms. Consequently, the aim of our paper is reached.

VI. Conclusion

In this paper, we studied a system that is composed of a VSI, an LC filter and a coupling inductor. We aim to enforce the output voltage of the studied system to track a reference voltage. To achieve this purpose, we designed a nonlinear controller using the backstepping technique. According to formal analysis and simulation results, the proposed controller allows a perfect tracking of the reference voltage and an asymptotic stability of the closed loop system. This asymptotic stability and that perfect tracking are obtained in grid connected mode with an undistorted grid voltage and with a distorted one and, also, in islanded mode.

Acknowledgment

The authors gratefully acknowledge the support of the Moroccan Ministry of Higher Education (MESRSFC) and the CNRST under grant number PPR/2015/36.

References

[1] M.R. Ebrahimi, M.N. Hashemnia, M. Ehsan and A. Abbaszadeh, “A novel approach to control the frequency and voltage of microgrids in islanding operation,” *IACSIT International Journal of Engineering and Technology*.,Vol. 4, No. 5, October 2012.

[2] H. Hua, L. Yao, S. Yao, S. Mei and G. Josep M, “An improved droop control strategy for reactive power sharing in islanded microgrid, ” IEEE Transactions on Power Electronics, 10.1109/TPEL.2014.2332181, 2015.

[3] M. S. Mahmoud, S. Azher Hussain and M A. Abido, “Modeling and control of microgrid: an overview,” *Journal of the Franklin Institute*,10.1016/j.jfranklin.2014.01.016. May 2014.

[4] A. A. Salam, A. Mohamed and M. A. Hannan, ”Technical challenges on microgrids, ” *ARPN Journal of Engineering and Applied Sciences*, VOL. 3, NO. 6, December 2008.

[5] S. Temel, S. Yağli and S. Gören, “P, PD, PI, PID controllers,” Middle East Technical University, Electrical and Electronics Engineering Department.

[6] D. Zammit, C. Spiteri Staines and M. Apap, “Comparison between PI and PR current controllers in grid connected PV inverters,” *International Journal of Electrical, Computer, Energetic, Electronic and Communication Engineering*. Vol. 8, No.2, 2014.

[7] T. Hornik and Q.C. Zhong, “A current-control strategy for voltage-source inverters in microgrids based on $H\infty$ and repetitive control,” *IEEE Transactions On Power Electronics*, Vol. 26, No. 3, March 2011.

[8] A. A. Ahmad, A. Abrishamifar and M. Farzi, “A New Design Procedure for Output LC Filter of Single Phase Inverters,” 2010 3rd International Conference on Power Electronics and Intelligent Transportation System. January 2010.

[9] G. Weiss, Q. C. Zhong, T. Green and J. Liang, “ $H\infty$ repetitive control of DC-AC converters in micro-grids,” Dept. of Electrical & Electronic Engineering. Imperial College of Science, Technology and Medicine. Exhibition Rd., London, SW7 2BT, UK.

[10] Y. A. R. I. Mohamed and E. F. El-Saadany, “Adaptive Decentralized Droop Controller to Preserve Power Sharing Stability of Paralleled Inverters in Distributed Generation Microgrids,” *IEEE Transactions On Power Electronics*, vol. 23, no. 6, Nov. 2008.

[11] E. Twining and D. G. Holmes, “Modelling grid-connected voltage source inverter operation, ” Power Electronics Group, Department of Electrical and Computer Systems Engineering, Monash University, Clayton.

[12] N. Pogaku and M. Prodanovi´c, “Modeling, Analysis and Testing of Autonomous Operation of an Inverter-Based Microgrid,” IEEE, 2007.

[13] M. Krstić, I. Kanellakopoulos and P. V. Kokotović, “Nonlinear and adaptive control design”, John Willy & Sons, NY, 1995.

ISSN 2356-5608

[14] H. El Fadil and F. Giri, "Nonlinear adaptive control for MPPT in photovoltaic systems, " *IFAC Proceedings Volumes*,vol. 42, issue. 9, pp. 392-397, ISSN 1474-6670.2009.
[15] N.H. Saad, "Backstepping nonlinear control strategy for dynamic voltage restorer using multilevel inverter," Conference Paper, 2014.
[16] A.Yahya, H. El Fadil, Josep M. Guerrero, F. Giri, H. Erguig, "Three-Phase Grid-Connected of Photovoltaic Generator Using Nonlinear Control", In Proceeding of the *2014 IEEE Multi-conference on Systems and Control (MSC-2014),* October 8-10, 2014. Antibes, France, pp. 879- 884.

ISSN 2356-5608